Developmental Cognitive Neuroscience 66 (2024) 101355

Contents lists available at ScienceDirect

Developmental Cognitive Neuroscience

journal homepage: www.elsevier.com/locate/dcn

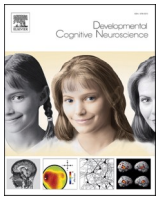

Multi-level fMRI analysis applied to hemispheric specialization in the language network, functional areas, and their behavioral correlations in the ABCD sample

Trevor K.M. Day [a,b,*], Robert Hermosillo [b,c], Gregory Conan [b], Anita Randolph [b,c], Anders Perrone [b], Eric Earl [d], Nora Byington [b], Timothy J. Hendrickson [b,e], Jed T. Elison [a,b,c], Damien A. Fair [a,b,c], Eric Feczko [b,c]

[a] Institute of Child Development, University of Minnesota, Minneapolis, MN, USA
[b] Masonic Institute for the Developing Brain, University of Minnesota, Minneapolis, MN, USA
[c] Department of Pediatrics, University of Minnesota, Minneapolis, MN, USA
[d] Data Science & Sharing Team, National Institute of Mental Health, Bethesda, MD, USA
[e] Informatics Institute, University of Minnesota, Minneapolis, MN, USA

ARTICLE INFO

Keywords:
FMRI
RsfMRI
Hemispheric specialization
Cortical specialization

ABSTRACT

Prior research suggests that the organization of the language network in the brain is left-dominant and becomes more lateralized with age and increasing language skill. The age at which specific components of the language network become adult-like varies depending on the abilities they subserve. So far, a large, developmental study has not included a language task paradigm, so we introduce a method to study resting-state laterality in the Adolescent Brain Cognitive Development (ABCD) study. Our approach mixes source timeseries between left and right homotopes of the (1) inferior frontal and (2) middle temporal gyri and (3) a region we term "Wernicke's area" near the supramarginal gyrus. Our large subset sample size of ABCD (n = 6153) allows improved reliability and validity compared to previous, smaller studies of brain-behavior associations. We show that behavioral metrics from the NIH Youth Toolbox and other resources are differentially related to tasks with a larger linguistic component over ones with less (e.g., executive function-dominant tasks). These baseline characteristics of hemispheric specialization in youth are critical for future work determining the correspondence of lateralization with language onset in earlier stages of development.

1. Introduction

Language serves not only its important communicative role, but also supports higher-order reasoning such as theory of mind (e.g. Ebert et al., 2017), and emotion regulation (e.g. Monopoli and Kingston, 2012). In the brain, language is processed by a left hemisphere-dominant network that comprises multiple regions thought to be specialized for distinct linguistic subskills.

This laterality has been found to increase between childhood and young adulthood (Holland et al., 2007; Lidzba et al., 2011; Sepeta et al., 2016; Szaflarski, Holland et al., 2006; Szaflarski, Schmithorst et al., 2006), and with increasing language skills within the same age range (Bartha-Doering et al., 2018), which may be due to a decrease in right hemisphere (RH) involvement (Dehaene-Lambertz et al., 2002; Olulade et al., 2020; Petitto et al., 2012). In older children, organization and laterality of the language network is not adultlike by 9 years (Enge et al., 2020; Skeide et al., 2014).

1.1. Challenges in investigating lateralization

Considering the drastic developments in language skills, the first few years of life are an important time period for understanding changes in cortical organization (Hervé et al., 2013; Johnson, 2001). Functional magnetic resonance imaging (fMRI), due to its high spatial resolution and non-invasiveness is well-suited to questions of cortical topology. However, using task-based fMRI (tfMRI) with infants and toddlers is difficult, as it relies on both the ability of the participants to effectively perform the task and lie very still. Resting state fMRI (rsfMRI) does not

* Corresponding author at: Institute of Child Development, University of Minnesota, Minneapolis, MN, USA.
E-mail address: day00096@umn.edu (T.K.M. Day).

https://doi.org/10.1016/j.dcn.2024.101355
Received 14 February 2023; Received in revised form 6 January 2024; Accepted 3 February 2024
Available online 8 February 2024

induce task demands, and is uniquely suited to the study of the development of functional brain organization and can even be conducted during natural sleep in infants (Dubois et al., 2021; Howell et al., 2018; Korom et al., 2022).

Resting state (RS) organization is individualized and accounts for a significant portion of task activation patterns suggesting it can be used to study online activation (Tavor et al., 2016). However, changes in the RS signal do occur over development: primary networks are further developed in neonates, compared to higher-order networks (Fransson et al., 2011; Gao et al., 2009, 2017) and become more dissimilar between individuals with age (Moore et al., 2023), which suggests that much of the infrastructure reflected by rsfMRI is in place early in development. Together, this suggests rsfMRI can recapitulate changes in task-response topology.

1.2. Using rsfMRI data to examine the development of the language network

MRI studies of language have been constrained by sample sizes (Bradshaw et al., 2017; Enge et al., 2020) that have been criticized for a lack of power (Button et al., 2013; Poldrack et al., 2017). Developing a new technique could prove problematic when using a small sample size by providing false-positive validation of an incorrect technique, so we leveraged the well-powered Adolescent Brain and Cognitive Development study (ABCD; Barch et al., 2018; Casey et al., 2018; Volkow et al., 2018) to develop and validate a novel technique for the study of lateralization using rsfMRI. Central to our assumption is that the cortical regions that support online language processing also vary together in RS and thus can be recapitulated using RS correlations (Biswal et al., 1995; Hermundstad et al., 2013; Mennes et al., 2010).

For these analyses we leveraged the MIDB Probabilistic Atlas that accounts for individual variability in our sample in network topology (Hermosillo et al., 2022). Specifically, we used regions of interest (ROIs) selected from the ventral attention network (VAN). The VAN is a RH-dominant exogenous attention network (Corbetta and Shulman, 2002) that closely mirrors the left hemisphere (LH)-dominant language network topologically (Bernard et al., 2020; Braga et al., 2020).

From this VAN, we used ROIs from inferior frontal gyrus (IFG) and middle temporal gyrus (MTG). MTG is thought to subserve morpho-syntactic and lexico-semantic categorization, lexical access, and phrase structure building (Skeide and Friederici, 2016), or to be involved non-selectively in a range of lexico-semantic as well as syntactic processing (Fedorenko and Blank, 2020). Our understanding of the role of IFG is in substantially more flux. One major line of work has argued the role of IFG in language is articulation (Broca, 1861; Flinker et al., 2015; Hillis et al., 2004; Long et al., 2016; Papoutsi et al., 2009). However, more recent work suggests IFG comprises subregions individually selective for language processing and another that is modulated by processing difficulty (Fedorenko and Blank, 2020; Weiss-Croft and Baldeweg, 2015).

1.3. Using rsfMRI to study the language network

In comparison to tfMRI literature, the rsfMRI literature is less mature. Researchers have used independent component analysis (ICA) to isolate the independent component most like a template. These studies so far have had small sample sizes (n = 15) and wide variation in overlap between individual-specific and canonical language networks (Branco et al., 2016; Smitha et al., 2019). While promising, such ICA approaches are affected by the number of components selected, cannot give region-level analyses, and bias the estimate toward the template, which was asymmetric in the former paper and symmetric in the latter. Likewise, Braga and colleagues (2020) used an iterative approach to refine a subject-specific ROI based on the qualities of its resulting seedmap and its similarity to the canonical language network. However, to re-apply such ROIs to the same timeseries would introduce data leakage.

This paper proposes and validates a new RS functional connectivity analysis specifically for the purposes of investigating for hemispheric specialization. We generate many seed-based connectivity maps meant to be representative of the language network, varying the relative proportion of LH and RH grayordinates in the seed region. This increases the reliability of our characterization of laterality by estimating the network multiple times. We demonstrate external validity by demonstrating a relationship between this technique and associations with behavioral tasks conducted outside of the scanner. Thus, it is informative with regards to brain-behavior associations and suitable for use across development, for example in infants and toddlers from whom only RS data was collected.

2. Methods

2.1. Participants

Data were taken from the ABCD baseline (Year 1) acquisition (ages 9–11 years). We used the ABCD Reproducibility Matched Samples (ARMS; Feczko et al., 2021), which are matched across the ABCD study based on site, age, sex, ethnicity, grade, highest level of parental education, handedness, combined family income, exposure to anesthesia, and family structure. Family members were kept in the same ARMS, and the ARMS were matched to have equivalent numbers of siblings, twin pairs, and triplets. Participants were included if they had more than 10 min of low-motion (framewise displacement < 0.2 mm) rsfMRI data, leaving 3098 individuals in ARMS-1 and 3055 in ARMS-2, see Supplementary Figure (SF) 2. The ARMS function as a within-study test/replication sample to increase our confidence in our findings by immediately performing a replication. Relative to the entire sample, the low-motion group is older, more female, more non-Hispanic white, and is more likely to have married parents, parents with graduate degrees, higher household incomes, has fewer mental and physical health problems, higher general cognition, executive functioning, and learning and memory scores (Cosgrove et al., 2022; Feczko et al., 2021), which limits generalizability.

While we modeled handedness as a continuous variable, we present the number of individuals in each handedness category based on the Edinburgh Handedness Inventory (EHI): left: EHI < -0.5; mixed: $-0.5 \leq$ EHI ≤ 0.5, right: EHI > 0.5 (Table 1, Veale, 2014).

Additionally, we divided the participants' linguistic environment (as reported in the ABCD Longitudinal Parent Demographics Survey; Barch et al., 2018) into the following mutually exclusive categories (Table 2), where each child was assigned to the most-bilingual-exposure category in which they fit. In this rating, we consider categories 3 and 4 "bilingual" (14%). There was no difference in distribution between ARMS, $\chi^2(4, 6153) = 3.988, p = .41$.

Each brain-behavior model was tested against demographic covariates, including gender, age, handedness, parental education, binned parental income (breaks: $2500, $8500, $14,000, $20,500, $30,000, $42,500, $62,500, $87,500, $150,000, $250,000), child anesthesia status, child race, and ABCD site.

Table 1
Number of individuals in each ARMS by handedness category (right: EHI > 0.5, left: EHI < -0.5, mixed: $-0.5 \leq$ EHI ≤ 0.5).

	Handedness n (%)		
ARMS	Right	Mixed	Left
1	2488 (80)	378 (12)	232 (7)
2	2476 (81)	376 (12)	203 (7)

Table 2
Number of participants in each category. Dual immersion was the "L2 in school" category. L1: first language; L2: second language.

Language Exposure	ARMS 1 N (%)	ARMS 2 N (%)
1. English at home and in school	2340 (76)	2244 (73)
2. English at home, L2 in school	152 (5)	158 (5)
3. Non-English home, child L1 is English	205 (7)	211 (7)
4. Child L1 is not English	228 (7)	247 (8)
5. Unknown	173 (6)	195 (6)

2.2. Preprocessing

Data were processed using the ABCD-BIDS processing pipeline (Sturgeon et al., 2021), which is a modified version of the HCP pipeline that is more general and compatible with the different MR platforms used across the ABCD study. This pipeline was previously described in detail (Feczko et al., 2021), and contains the HCP pipeline steps of PreFreeSurfer (with the modification of allowing a missing T2), FreeSurfer, PostFreeSurfer (conversion to CIFTI), fMRIVolume, fMRISurface (registration), and the additional steps of DCAN BOLD processing, and Executive Summary creation.

2.3. Network level results

2.3.1. Network creation

For a complete description of the generation of the template matching (TM) maps used in this paper, see Hermosillo et al. (2022), which implements methods from Gordon and colleagues (2017). Briefly, for each subject, a network assignment was generated for each grayordinate based on the similarity of spatial pattern of functional connectivity to an independent set of network templates. Then, each cortical and subcortical grayordinate was assigned a likelihood of belonging to each of 14 networks across the group. Those networks were the default mode network (DMN), the visual network (VIS), the frontal parietal network (FPN), the premotor network (PMN), the dorsal attention network (DAN), the ventral attention network (VAN), the salience network (Sal), the cingulo-opercular network (CO), the sensorimotor dorsal network (SMd), the sensorimotor lateral network (SMl), the auditory network (AUD), the temporal network (MTL), parieto-occipital network (PON), and the parietal medial network (PMN).

Ten minutes of data with a framewise displacement (FD) of less than 0.2 mm were sampled from each subject, and the probability of network observation (η^2) is calculated for each network. Network templates were initially created in ARMS-3, the small, held-out development set of ABCD participants (Feczko et al., 2021). η^2 values are calculated by correlating the template dense time series across all grayordinates within a session. Whole-brain connectivity at each grayordinate was thresholded to Z-scores greater than or equal to one (independently within hemisphere, subcortex, and cortex-to-subcortex). The correlation between this suprathreshold map and each template is theη^2. Each grayordinate is assigned to the network with the maximum η^2, i.e. a "winner-take-all" approach. Finally, some clean-up, including hole-filling, is performed after binarization to create assignments for each network for each subject.

2.3.2. Characterizing networks

First we calculated a network binary LI (bLI), using the classic LI formula $LI = \frac{L-R}{L+R}$, where L and R are the number of in-network vertices in each hemisphere. Secondly, binarization of η^2 obscures information about the underlying probability of network observation. In other words there is no distinction between these two scenarios: (1) a clear correct assignment, where the highest η^2 is much greater than all others; and (2) a vertex where there is no clear winner, and multiple networks may be detectable, e.g. at the edge of a network, yet one must be selected.

We explored two methods of comparing grayordinate-wise η^2values in an attempt to be more sensitive to the underlying distribution of η^2 values, a continuous LI (cLI), where the left and right η^2 values were subtracted from one another pairwise, and a *t*-test LI (tLI), where the vectors of left and right η^2 were treated as paired estimates.

Initially, we calculated cLI. In order to do this, because the grayordinate CIFTI matrix is not symmetric, we projected the LH values onto the RH, so that values can be paired. Then, we simply subtracted the projected RH η^2 values from their corresponding LH value, resulting in 29,706 difference values for each network. The average voxelwise difference across the brain is thus the cLI. As only positive template probabilities were assigned, the theoretically largest possible difference is 1 or − 1, representing perfect left or right dominance, placing it on the same scale as bLI, however cLI ranged mostly between 0.1 and −0.1.

As this model of the cortex in this framework pairs values across the hemispheres, we can also perform a paired *t*-test to distinguish more intricately between hemispheres (tLI), although due to the large sample size (29,706) the test itself is often trivially significant, and so we report effect sizes (Cohen's d). Because cLI and this metric tLI are so highly correlated ($r = 0.92$ across all individuals and networks), we just use tLI going forward. It is important to note that, just as a grayordinate does not represent the signal from a meaningful grouping of neurons (other than adjacency), pairing of values across the central sulcus this way matches values only homotopically, not homologously, and so a tLI takes into account both the greater extent in one hemisphere — spatial asymmetry — and underlying differences in the confidence of network assignment.

Secondly, because the ipsilateral connectivity bias theoretically causes extraneously elevated correlation coefficients between language areas and non-language areas, our method controls for this bias by evaluating the laterality of the language network estimate against the laterality of the seed.

2.4. The integrated laterality index

2.4.1. ROI selection

The optimal method to create a session-level ROI would be using an approach similar to that of Braga and colleagues (2020), by identifying what ROI creates a language-network-like seedmap. However, applying such an ROI to the data it was created from would introduce data leakage and circularity issues, and we long enough fMRI scans to split a single session in half across the ABCD sample to both create and apply an ROI. Thus, we decided on a technique that would maximize the overlap of the selected ROI across participants without introducing data leakage. We leveraged previous work on ABCD to identify regions of cortex that are reliably found to host the VAN in ABCD.

The VAN is a consistently identified cortical network (Gordon et al., 2016; Hermosillo et al., 2022; Power et al., 2011; Yeo et al., 2011) that seems to comprise a LH language network and RH attention network (Bernard et al., 2020; Lee et al., 2012). We used the VAN map described above, and began by thresholding it at 0.5 probability (i.e. all grayordinates that were present in at least 50% of participants). We used the large inferior frontal region from this map as our IFG ROI, see Fig. 1. Qualitatively, we noticed that MTG segregated into a large ventral component and a smaller anterior component at a slightly higher threshold of 0.586 in LH. In this analysis, we term the larger component "MTG" and the smaller "Wernicke's area" (WA) based on its location near the temporoparietal junction, similar to Tremblay and Dick's (2016) definition, although much smaller in extent (see Fig. 1). We created ROIs for both ARMS, but they were so spatially similar that we used ROIs from ARMS-1 in analyses of both ARMS for consistency. This method only identified the three regions discussed above, and did not identify that other regions important for language were consistent enough within the sample to pass the threshold for inclusion, such as the middle frontal gyrus, superior temporal gyrus, temporal pole and ventral temporal lobe.

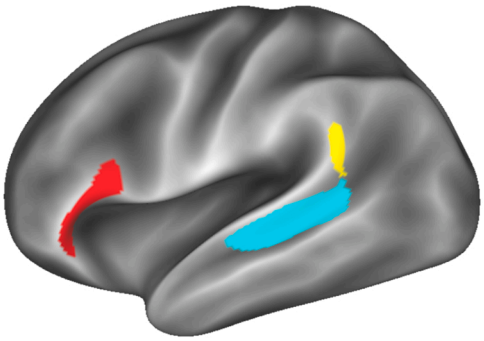

Fig. 1. The surface-based ROIs selected for this analysis. Red: inferior frontal gyrus (IFG); blue: middle temporal gyrus (MTG); yellow: "Wernicke's area." Only the LH is shown because left ROIs were projected onto the RH for all analyses.

The left ROIs were uniformly larger than the right (IFG L: 351 grayordinates, R: 177; MTG L: 490, R: 482). Indeed, there was no right-hemisphere Wernicke's ROI at this threshold (L size: 81). We projected all canonical left ROIs onto the right hemisphere for the next step, creating *homotopes*, rather than using the functional *homolog*. This was necessary to facilitate our analysis, as described below, that swaps out left for right vertices as necessary.

Our three ROIs overlap spatially with Fedorenko's Language Atlas (Lipkin et al., 2022), providing external validity for our ROI selection (see SF 6.1), however, some mismatch in temporoparietal junction is evident, as is the inclusion of non-language IFG, which possibly impacted our results.

For all three conceptual ROIs, we created sets of CIFTI ROIs that incorporated n_L grayordinates from the canonical left ROI and n_R grayordinates from the mirrored ROI, where n_L and n_R sum to equal the total size of the left ROI ($n_{\max}$). For each value of increasing n_R between 1 and ($n_{\max} - 1$), we randomly selected n_R grayordinates to involve from the right ROI, and removed the corresponding grayordinate from the left, see Figure LLL(a). We repeated this process 10 times for each value of n_R, so that later steps can randomly select a pregenerated bilateral seed out of 10, rather than creating a new one during processing. These seeds are available on Zenodo (https://doi.org/10.5281/zenodo.7289743). We refer to the proportion of right-hemisphere grayordinates relative to the ROI as *seed laterality* (SL), however remapped such that $n_R = 0$ receives an SL value of 1; and $n_R = n_{\max}$ a value of -1. Therefore, a seed with equal proportions left/right has an SL value of 0. This sign convention follows the laterality literature in representing LH with positive values.

2.4.2. Seed maps

For increasing values of n_R, we used as a source ROI for the DCAN Lab Seed Map Wrapper (link: https://gitlab.com/Fair_lab/Cifti_conn_matrix_to_corr_dt_pt), which generates a whole-brain correlation map. For each map, we used exactly 10 min of low motion (FD $<$ 0.2 mm) data randomly sampled from available data, removing motion outliers, and performed *r*-to-*Z* transformation on the result (Figure LLL(b-c)). For images of the *r*-value maps, see SF 3b.

We calculated an LI for each seed map, using *wb_command -cifti-find-clusters* with a *Z* threshold of 0.4 and a surface area threshold of 10 mm^2 to remove only the most spurious areas of correlation and *wb_command -cifti-stats* to count the number of surviving grayordinates in each hemisphere. Then we calculated the LI as $LI = \frac{L-R}{L+R}$ (Figure LLL(d)). Although there is technically a different number of grayordinates in each hemisphere in the CIFTI matrix, the difference is small enough to make no difference in the overall LI calculation.

Seed maps with more-rightward SL were on average slightly smaller (IFG $\beta_1 = -3.55$, $\beta_2 = -3.52$ grayordinates per percentage point increase in SL, values for both ARMS given in subscript; Wernicke's $\beta_1 = -0.991$, $\beta_2 = -0.873$; MTG $\beta_1 = -1.97$, $\beta_2 = -2.05$, all p values $<.001$).

2.4.3. Integration

Initially, we calculated laterality indices using all $10 \times n_{\max}$ possible seed maps (e.g. for IFG, 3510). However, visual inspection of the results demonstrated that the clustering of the points along a polynomial line of best fit ($R^2 > .99$; SF 3a) showed that using multiple replicates at each SL value was unnecessary. In order to reduce computation time, we used 100 seed maps per session to calculate ILI, using random selection of one out of the 10 pre-hoc ROIs for each SL, which performed well relative to the best-estimate using seedmaps at each n_R value, see Supplementary Material 3. For WA, which was smaller than 100 grayordinates, all values of n_R were included.

Across all participants, the LI trend was clearly not linear. We performed a simple ANOVA model selection approach to select the best functional form to use across sessions. We randomly selected 100 sessions (50 from each ARM) and fit polynomial models between linear and quintic, inclusive. The most frequent best functional form was a cubic ($n = 29$), with the other models being selected as the best-fitting form with the following frequencies: linear: 4, quadratic: 26, quartic: 25, quintic: 16. The median best-fitting model was the cubic. Furthermore, there is no theoretical reason to suggest that the laterality of these mixed estimates of language function laterality would uniformly approach one extreme more rapidly than the other, thus a symmetric function like a cubic is consistent with how we might expect the estimate to behave relative to biology. That said, all models performed very well (mean R^2 linear: 0.963; quadratic: 0.989; cubic: 0.992; quartic: 0.993; quintic: 0.993). Visualizations of some example trends can be found in Supplementary Material 3.

From this curve, there are a number of estimates that become immediately apparent: the *y*-intercept,[1] the value at SL = -1 and 1, as well as the *x*-intercept. The *x*-intercept in particular is not always interpretable, as it does not always occur between $-1 <$ SL < 1, and cubics can have multiple *x*-intercepts. The extreme SL values, of course, reflect the laterality of language activity alone as it relates to a single ROI, and thus does not avoid theipsilateral effects we set out to control for.

Thus, we chose to calculate the integral of the cubic fit, creating an *integrated laterality index* (ILI). The correlation between these values and the integration of the cubic fit are presented in Table 3. Notably, the two most interpretable parameters (*y*-intercept and ILI) are at unity, however, as we will show, ILI has better predictive value for behavior. In the below analysis, the smallest root of the polynomial was taken as the *x*-intercept.

Fig. 2 shows the processes of calculating an ILI for a non-lateralized participant. First, (a) shows a mixed source ROI; (b) shows the resulting seedmaps at different mixing percentages (75% left, 50%, and 25%); (c) shows the resulting laterality indices based on 100 samples of source ROIs; and finally (d) shows the cubic fit as it changes based on the source

Table 3
The correlation between values extracted from cubic fits. ARMS 1 on the left, ARMS 2 on the right. All *r* values are trivially significant at large *n*.

	Value			
Value	1	2	3	4
1. *y*-intercept				
2. *x*-intercept	.73 /.70			
3. SL = 1 (L)	.22 /.25	.43 /.41		
4. SL = −1 (R)	.37 /.36	.13 /.12	-.36 / − .36	
5. ILI	.97 /.97	.76 /.72	.41 /.44	.40 /.38

[1] Here is where the value of remapping n_R becomes useful, as the *y*-intercept now represents equal sampling from both hemispheres.

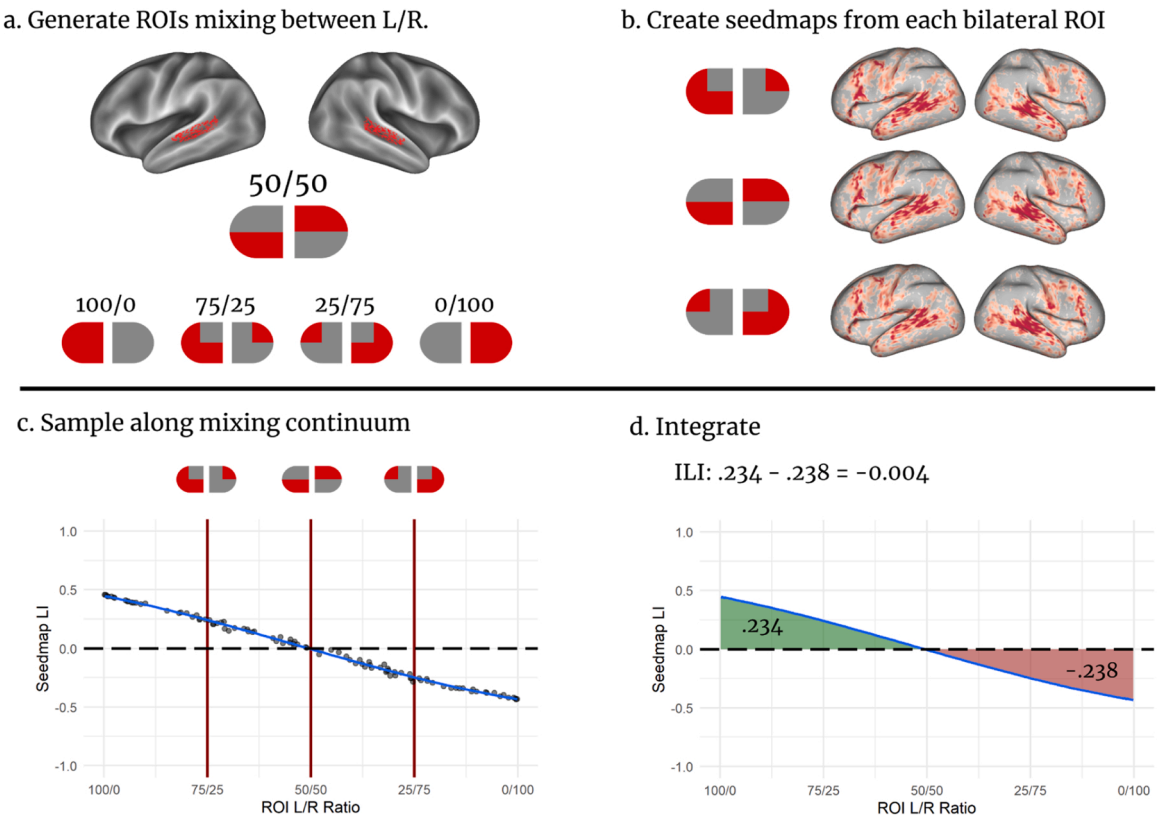

Fig. 2. Graphic representation of ILI creation. (a) Bilateral ROIs including grayordinates from both hemispheres are created, by removing n grayordinates from the left ROI and adding n matching homotopic ROIs from the RH. (b) Seedmaps are created from each bilateral ROI. Example seedmaps from a non-lateralized participant are shown for ROIs containing 75%, 50%, and 25% LH voxels. (c) Mixing proportions are sampled between 100% and 0% LH to create a regression line (blue). The same proportions and individual as (b) are shown. (d) The area under the curve (cubic fit) is calculated; resulting in the "ILI." The same individual is shown in each subfigure and the areas under the curve are highlighted.

ROI, showing this individual had high degrees of ipsilateral connectivity, but that the underlying network trends toward bilaterality.

After Benjamini-Hochberg correction, there was a statistically significant relation between mean seed map size and ILI for IFG in both ARMS ($\beta_1 = 0.0000249$, $\beta_2 = 0.0000250$, $p_1 < .001$, $p_2 < .001$), but not for MTG ($p_1 = .527$, $p_2 = 0.410$) or WA ($p_1 = .197$, $p_2 = 0.414$).

Across both ARMS, ILI_{IFG} and ILI_{MTG} were significantly (all $p < .001$, one-sided *t*-test) left-lateralized, but ILI_{Wer} was significantly right-lateralized (both ARMS $p < .001$), see Fig. 3(a). Example MTG seedmaps for a left-lateralized participant ($Z \approx 2$) and a right-lateralized participant ($Z \approx -2$) are shown in Fig. 3(b), see Supplementary Materials 3 for more details.

2.4.4. Behavioral and environmental characteristics

We examined the specificity of the relationship between ILI and not only language-related behavior measures, but with all behavioral scores previously analyzed in ABCD by Thompson and colleagues (2019). These include all seven subscores from the NIH Toolbox (Bauer and Zelazo, 2014; Weintraub et al., 2013), as well as the Little Man Task (LMT; Ratcliff, 1979) and the Rey Auditory Verbal Learning Test (RAVLT; Lezak, 1983).

Under the differentiation hypothesis, the underlying structure of cognition changes from childhood into adolescence (Mungas et al., 2013; Shing et al., 2010; Thompson et al., 2019), and to that end, we investigated two sets of composite scores measuring latent components of cognition. The first set are the sum-score composites from the Toolbox: Total Composite (TC; all instruments), Crystallized Composite (CC), and Fluid Composite (FC), see Table 4. We additionally included the three principal component (PC) scores described by Thompson and colleagues: General Ability, Executive Function, and Learning & Memory. These scores will be referred to as *PC1-GA*, *PC2-EF,* and *PC3-LM*. Although PC scores are calculated with all instruments, each instrument is listed with the PC(s) where its weight was greater than 0.4.

The majority of participants had behavioral assessment and MRI acquisition on the same day (77%), with 22% of participants doing the MRI acquisition within the month following behavioral assessment, and 1% doing the MRI within the month before behavioral assessment. Less than 1% of the total sample had more than a month between assessment and acquisition.

2.5. Brain-behavior correlations

In the models below, we included child age in months, child grade, highest parent education in years, parent income (as factor), child gender, child anesthesia exposure (yes/no), child race,[2] and site as covariates. We independently tested for an effect of handedness as it is of substantive interest in laterality effects. Including handedness, these are the variables originally used to balance the ARMS, and tests were conducted independently in each ARMS to achieve test-retest reliability.

We also examined the effect of linguistic exposure on laterality. To simplify, we examined the difference between monolinguals (Group 1) and bilinguals (Groups 3 and 4), leaving out the relatively small dual-immersion-only group (Group 2). There was no difference in laterality between language exposure groups, except in bLI in ARMS2 ($p = 0.038$ following Benjamini-Hochberg [BH] correction), so we do not include linguistic exposure in models going forward.

[2] White, Black, Native American/Alaskan Native, Native Hawaiian/Pacific Islander, Asian, more than one, other

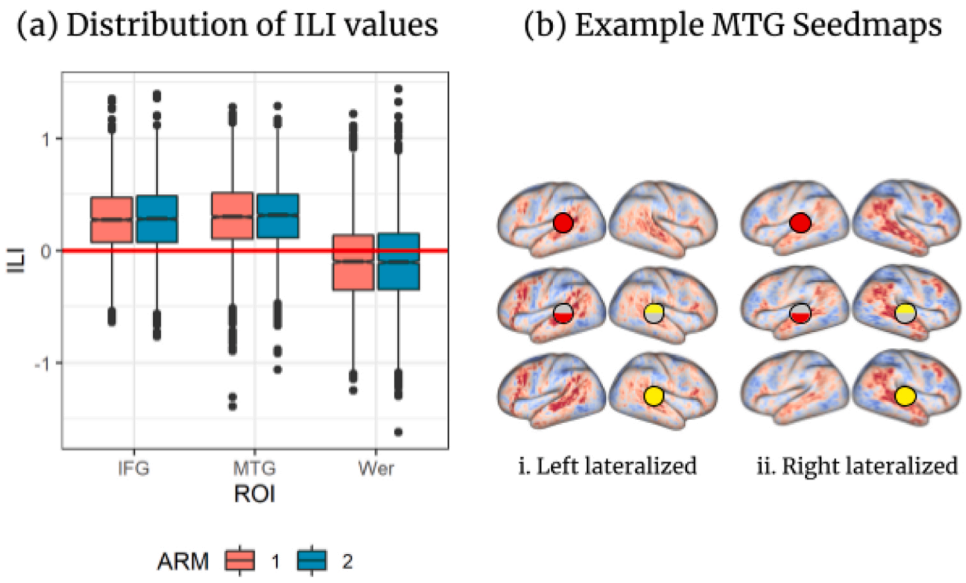

Fig. 3. (a) Distribution of ILI for all three ROIs in both ARMs (1: red, 2: blue). Wer: Wernicke's area. (b) Example seedmaps for two participants at source mixing percentages of (top to bottom) 100% left, 50/50%, and 100% right, indicated with schematized ROI representations. Participants are (i) strongly left-lateralized and (ii) strongly right-lateralized).

Table 4
List of all behavioral measures included in the analysis, including the short form of their name, their Toolbox composite score (sum score) and their weights onto Thompson PCs that exceed 0.4. All NIH-TB instruments are included in the Total Composite.

Instrument	Short Name	NIH Composite	Thompson PC (weights > 0.4)
NIH-TB			
Picture Vocabulary	Pic Vocab	Crystallized	PC1-GA (.754)
Oral Reading Recognition	Reading	C	PC1-GA (.820)
Dimensional Card Sort	Card Sort	Fluid	PC2-EF (.710)
Flanker Inhibitory Control and Attention	Flanker	F	PC2-EF (.712)
Picture Sequence Memory	Picture	F	PC3-LM (.863)
List Sorting Working Memory Test	List	F	PC1-GA (.471)
Pattern Comparison Processing Speed	Pattern	F	PC2-EF (.813) PC3-LM (.493)
Others			
Little Man Task	LMT	-	PC1-GA (.500)
Rey Auditory Verbal Learning Test (Immediate Recall)	RAVLT	-	PC3-LM (.712)

Rather than testing our brain measures against only relevant behavioral measures, we instead show the effect of laterality on the 15 behaviors listed above (NIH Youth Toolbox, Little Man Task, RAVLT, and Thompson PC scores), providing external validity and specificity. We separate all analyses by ARMS to provide immediate, within-study replication.

3. Results

3.1. Network laterality scores are associated with each other and handedness, but not linguistic exposure

The original networks were calculated from a set of 6066 participants across both ARMS. The bLI ranged from [− 0.65, 0.864] and tLI from [− 0.62, 0.61], but the first is bound [−1, 1] and the latter unbound (an effect size). The correlation between the two metrics is $r = 0.79$, but correlation varied by network, between [.52,.86]. Notably low were the correlations between LIs in the MTL, perhaps reflecting low confidence in the probabilistic assignments in that network, likely due to the susceptibility weighted artifact common in the mesial temporal lobe (e.g. Olman et al., 2009). Accordingly, the TP network was the second-lowest. In our network of interest, the VAN, correlations were approximately $r = 0.78$ (Fig. 4).

There was an association between handedness score and bLI ($\beta = 0.021, p < .001$) after controlling for the covariates listed above, with the effect that the average entirely right-handed participant had a bLI 0.042 units more lateralized than the average entirely left-handed participant, which approximates a Cohen's d of 0.4. There was likewise an effect on tLI ($\beta = 0.015, p < .001$), with the effect that the average entirely right-handed participant had a tLI 0.030 units more lateralized than the average entirely left-handed participant, which approximates a Cohen's d of 0.3. In both scores, the average left-handed LI was greater than zero, i.e. still left-lateralized.

3.2. tLI, but not bLI is associated with behavior scores

Each estimate is the single beta weight for the laterality metric, controlling for the variables mentioned above (including handedness score). We differentiate point estimates of beta weights by p-values in Fig. 5, those greater than 0.05 (gray) and those that survive correction (red).

In Fig. 5, the behaviors are standardized and ordered by average beta weight across ARM and metric (bLI/tLI). The same order is used on both facets. We note a general increase in weight as the linguistic skills needed for the behavior increase; e.g. Toolbox Reading and RAVLT-Immediate scores are among the highest. bLI showed fewer significant associations; with no behavioral task showing replicable associations after BH correction for 60 multiple comparisons.[3] Using tLI, PC1-GA, Toolbox Crystallized Intelligence, Toolbox Reading, and RAVLT were significant in both ARMS. Models evaluating the effect of all network laterality on all behaviors can be found in Supplementary Material 4.

Finally, due to the high correlation between ILI and the y-intercept of the cubic fit, we examined the explanatory power of ILI compared to the y-intercept (i.e., the 50–50 ROI), and the left and right ROIs. Uniformly across behaviors, ILI explained a higher proportion of the behavior than the left ROI, which explained more of the behavior than the 50/50 ROI.

[3] Fifteen behaviors × two ARMs × two LIs

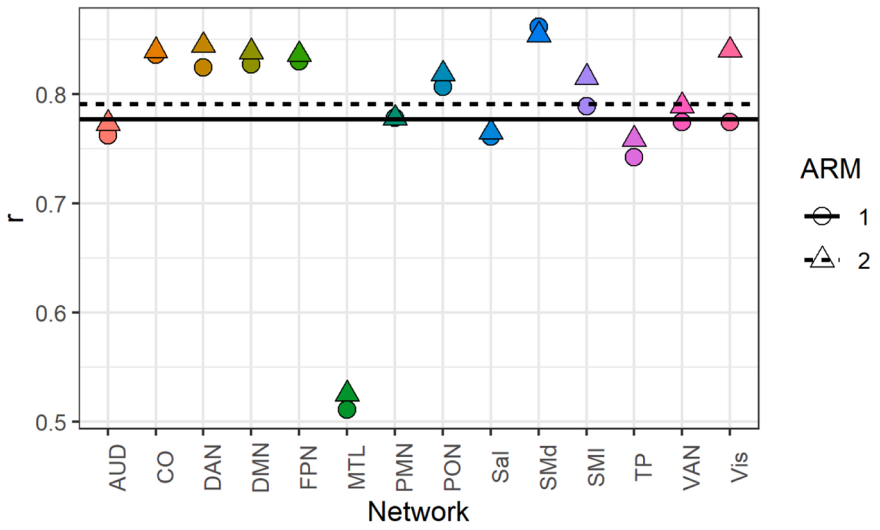

Fig. 4. Correlations between bLI and tLI across networks, by ARM. Average correlation by ARM shown with solid (ARMS-1) and dashed (ARMS-2) lines. Points are colored by network. Correlations are notably low in the MTL, perhaps reflecting low confidence in the probabilistic assignments in that network, likely due to the susceptibility weighted artifact common in the mesial temporal lobe.

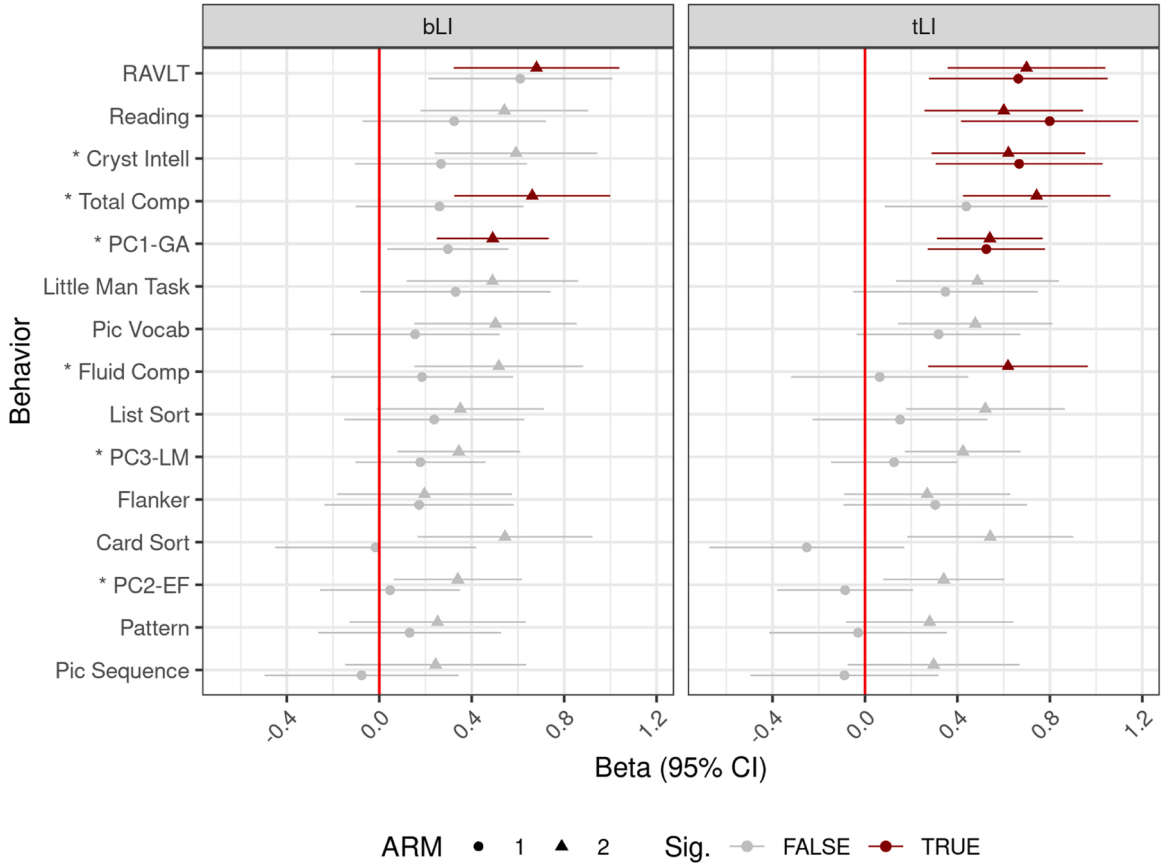

Fig. 5. Beta weights for behavior-brain associations for both LIs. Horizontal ranges represent 95% CI. Associations significant after BH correction in red, non-significant in gray. ARMS-1 in circles, ARMS-2 in triangles. On the y-axis, composites prefixed with an asterisk.

Rarely did the laterality associated with the right ROI explain a significant proportion of the variance (only in MTG AMRS-1 and in PC1-GA, Toolbox CC, and Toolbox Reading), see SM 5.

Importantly, this also demonstrates a non-reliance of the summary measure on laterality changes associated with the RH, which is a mechanism that has been proposed in children younger than the 9–11 year old participants in this study (Dehaene-Lambertz et al., 2002; Enge et al., 2020; Olulade et al., 2020; Perani et al., 2011; Petitto et al., 2012).

3.3. ILI is not associated handedness or linguistic exposure

We tested handedness and linguistic exposure for ILI as well. The effects of handedness on ILI_{IFG} were not significant. Handedness had an effect on ILI_{MTG} in ARMS-2 ($\beta = .281, p = .002$, but not ARMS-1 ($\beta = .$

602, $p = .158$). The effect was significant in both ARMS for ILI_{WA}, but in opposite directions (ARM1: $\beta = 0.272, p < .001$; ARM2: $\beta = -0.172$, $p < .001$), all p-values BH corrected for multiple comparisons. Because the effects of handedness on ILI do not replicate between ARMS, we consider this to indicate correlations with handedness are spurious. Likewise, controlling for covariates, there was no effect of bilingual status on any ILI, so linguistic exposure is not included in future covariates. The partial correlation between ILIs was IFG-WA: 0.18 - 0.22; IFG-MTG: 0.42 - 0.43; WA-MTG: 0.14 - 0.17 (values for both ARMs shown).

3.4. ILI for MTG is associated with behavior, but not IFG or WA

We present a similar behavioral plot for ILI measures. In IFG and MTG, the association between behaviors and ILI increased as the amount of linguistic skill needed for the task increased (Fig. 6). No patterns emerged for WA, so we will discuss IFG and MTG. Below, we present statistics for individual models predicting neurobehavioral outcome against demographic variables and ILI, following BH correction for 90 multiple comparisons.[4]

Between IFG and MTG, associations were significant in both ARMS for the RAVLT, Toolbox Pic Vocab (only in MTG), Toolbox TC, Toolbox Reading, Toolbox CC, PC1-GA. The LMT and Toolbox List Sort tasks were significant in both ARMS for MTG, but not IFG.

3.5. Multilevel Analysis

One of the goals of this project was to assess laterality of language function through the lenses of network-level laterality (bLI, tLI) and the lateralization of functional regions (ILI_{IFG}, ILI_{WA}, ILI_{MTG}). To this effect, we must examine whether these different metrics explain different components of the outcome.

Due to the large correlation between the network metrics (bLI/tLI: $r \approx 0.8$), and because bLI was not consistently associated with any of the behavioral outcomes, we use tLI to examine network laterality. Likewise, while ILI_{WA} was not associated with any metric and ILI_{IFG} was not reliably associated with any metric, we only examine ILI_{MTG}, which was reliability associated with PC1-GA, Toolbox CC, Toolbox Reading, Toolbox TC, and the RAVLT.

We fit nested models on the five behavioral measures reliably predicted by ILI_{MTG} (see above) to understand whether network- and ROI-level laterality explain distinct elements of the outcome. We performed ANOVAs on the null model (demographic predictors only), a second-level model model incorporating network laterality, and a third-level model additionally incorporating MTG laterality. The AIC for these sets of models are shown in Table 5; all improvements are significant for PC1-GA, Toolbox CC and Toolbox Reading. Toolbox TC and RAVLT showed no reliable improvement adding either the network-level or ROI-level laterality, i.e. the only significant improvement was in ARMS-2 demographics-to-network.

4. Discussion

Laterality of functions could be an important bioindicator of neurodevelopment and ongoing cortical and hemispheric specialization in young children. Many important skills have most frequently been indexed with tasks — either due to the study population or aims — but routine collection of RS data in addition to study aims has become increasingly common. Therefore, we developed a new RS technique to characterize the laterality of the language network using ROIs known to participate in the adult language network, allowing examination of those data without an in-scanner language task. Our method may also extend to other areas demonstrating HS, such as visual word form detection and face processing.

Generally, we found that associations between our network-level and ROI-level brain measures and behavior were larger for tasks requiring language-specific, rather than domain-general skills. This is true even in the analyses where task-laterality relations did not meet statistical significance.

4.1. Linguistic tasks show the largest associations

It is not common to report the lack of association between brain measurements and instruments that should *not* be associated with the outcome of interest. Previous fMRI studies (Hwang et al., 2019) and studies on the ABCD behavioral data (Dick et al., 2019) studies have examined relevant parts of the Toolbox, but not necessarily discriminant validity. Other fMRI studies have examined external validity with the Oral and Written Language Scales (Carrow-Woolfolk, 1996; Szaflarski, Schmithorst et al., 2006) and verbal IQ as measured by the Wechsler Abbreviated Scales of Intelligence (Bernal et al., 2018; Everts et al., 2009; Wechsler, 2014), but not contrasting instruments. By far, most fMRI studies rely on performance based on in-scanner tasks for validity, rather than behavioral instruments collected outside of the scanner (e.g. Joliot et al., 2016; Smitha et al., 2017; Szaflarski, Holland et al., 2006; Tzourio-Mazoyer et al., 2016; Zago et al., 2016).

Lacking in-scanner tasks, we were forced to rely on out-of-scanner tasks. However, we aimed to demonstrate validity by showing that our ILI is associated more highly with behavioral metrics involving language skills, and less to not at all with metrics not involving language skills. Our results support this pattern. We succeeded in demonstrating this with laterality associated with MTG, but did not find laterality associated with IFG to be more highly associated with language skills over all others.

To summarize, we reported on five analyses: two ways of measuring network-level laterality across the entire cortex and laterality associated with three language ROIs. Except for "WA," the tasks most frequently appearing with the highest beta values were Toolbox Reading, Toolbox Picture Vocabulary, the RAVLT, and the composite score Toolbox CC (the linear combination of Reading and Pic Vocab), as well as two other composite scores: Toolbox TC, and PC1-GA. The laterality associated with the MTG specifically, rather than the VAN at large explained more of the variance for Toolbox Reading, Toolbox CC, and PC1-GA, but not Toolbox TC, and the RAVLT. This may reflect the more domain-general skills invoked in the latter tests, namely all the fluid scores and the increased memory demands of the RAVLT over the other tasks (which require no memory beyond the trial).

The "WA'' ROI showed no patterns of association. As can be seen in SF 6.1, while our ROI is contained within the extent of the language network as defined by Lipkin and colleagues, it also misses a considerable amount of the area identified by those authors as involved in the language network. Its small size also indicates a low amount of inter-subject spatial reliability, and as mentioned, there was no RH homolog, thus we consider that under our method of ROI creation, this area captured more irrelevant cortex within individuals. For example, the mixed seedmaps that include LH language areas and non-language RH areas would not be very lateralized, and thus the variance of the laterality scores would be meaningless when regressed against behavior variance.

Regarding the IFG analysis, the results show a trend consistent with an understanding of the IFG as containing distinct language and domain-general sub-regions. Because our ROI was large, to capture the IFG across more than 6000 individuals, our brain-behavior results do not show high degrees of specificity for language, as it may have captured both language and domain-general sub-regions. Even then, there is large heterogeneity in topology (Gordon et al., 2017; Hermosillo et al., 2022; Keller et al., 2022) that dampens the usefulness of ROIs applied across individuals. Likewise, Moore and colleagues (2023) demonstrated that, although adultlike resting state networks exist in infancy, networks are

[4] Fifteen behavioral scores × three ROIs × two ARMs

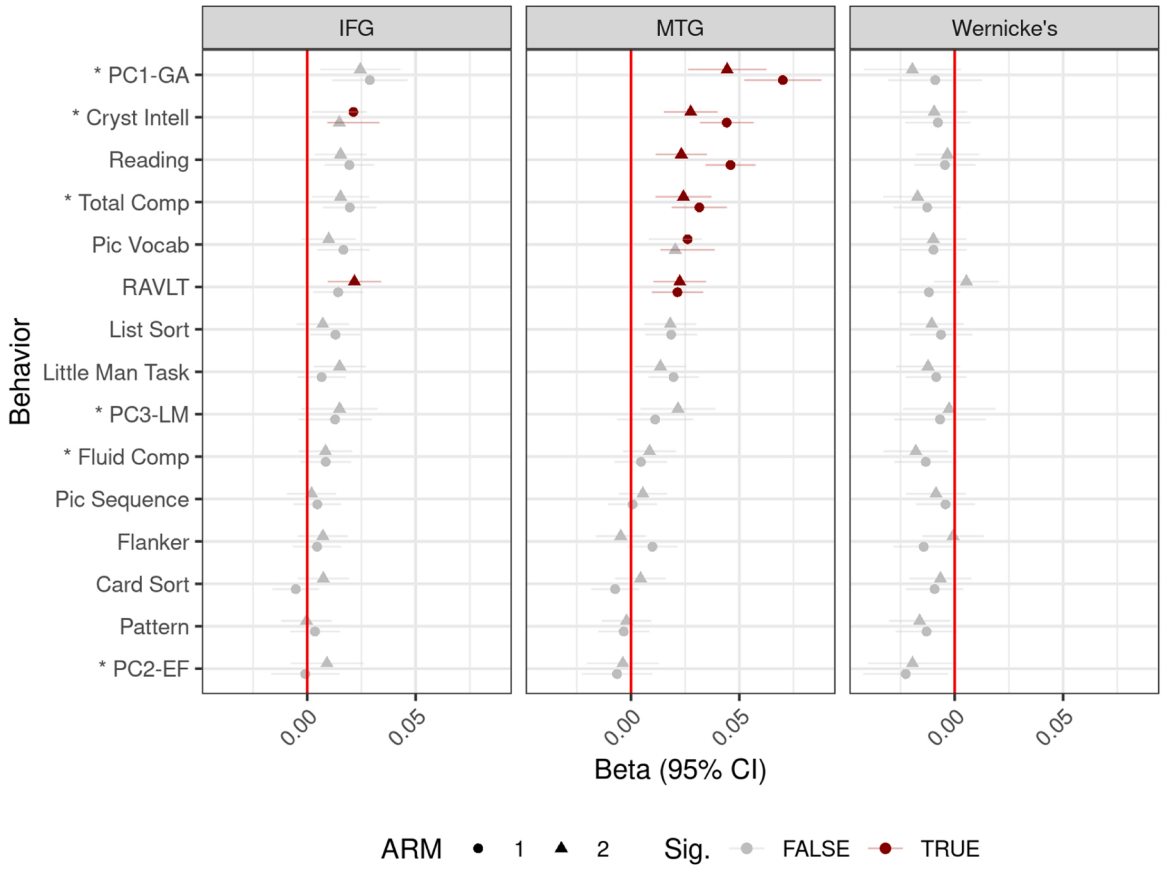

Fig. 6. Beta weights for behavior-brain associations in all three ROIs. The vertical line shows no relation between brain/behavior. Horizontal ranges represent 95% CI. Associations significant after BH correction in red, non-significant in gray. ARMS-1 in circles, ARMS-2 in triangles. On the y-axis, composite scores are prefixed with an asterisk. Note the different order from the previous plot.

Table 5
Information criteria for six nested models predicting three behaviors from both ARMS. DOF and p-values in columns 1 and 2 show values for the test comparing the current model to previous. P-values Benjamini & Yekutieli corrected for 20 correlated multiple comparisons. The DOF for all tests was 1.

		Model		
Behavior	ARMS	*0. Demographics*	*1. Network* DOF= 1	*2. Network + MTG* DOF= 1
PC1-GA	1	4094	4079 $p < 0.001$	4068 $p = 0.002$
	2	4469	4450 $p < 0.001$	4442 $p = 0.007$
Toolbox CC	1	5890	5879 $p = 0.002$	5871 $p = 0.008$
	2	6582	6571 $p = 0.002$	6564 $p = 0.008$
Toolbox Reading	1	6342	6327 $p < 0.001$	6310 $p < 0.001$
	2	6940	6931 $p = 0.004$	6925 $p = 0.014$
Toolbox TC	1	5759	5755 $p = 0.069$	5755 $p = 0.847$
	2	6369	6349 $p < 0.001$	6349 $p = 0.565$
RAVLT	1	6340	6331 $p = 0.006$	6332 $p = 1.000$
	2	6866	6852 $p = 0.001$	6853 $p = 1.000$

continuing to differentiate through adolescence, which likewise limits the applicability of a single ROI applied against individuals.

However, the relative simplicity of the tasks that do not reflect higher-order syntactic processing that is also consistent with IFG as a syntactic node: If the asynchronous linguistic tasks do not index syntactic processing, then it would likewise show small-to-no effects in the syntactic node. Future research - such as in the Human Connectome Project - should analyze subject-specific, task-localized, language-selective IFG nodes in order to dissociate domain-general signal.

Language is only one facet of cognition, and even those Toolbox tasks with more language components don't rely on language alone. Cognitive skills do not exist in isolation, and composite scores decrease method variance that can emerge from using a single task. Therefore, it is not surprising that some composite scores emerge as having higher associations with laterality than single-task measurements, based on the relative amount of noise in each measurement. This is especially true for Toolbox CC, which is a linear composite of the two language tasks.

In both IFG and MTG, we also find that the smallest beta values were found for the Toolbox Flanker, Toolbox Card Sort, and Toolbox Pattern Matching tasks. This pattern suggests that the laterality of the language network in adolescents is differentiably associated with language-specific, rather than domain-general executive function skills, however the effect sizes for IFG are perhaps decreased by the inclusion of domain-general processing subregions.

Together, this pattern shows that our laterality measure indexes the appropriate behaviors, and is not associated with behaviors reliant on other aspects of cognition. If we were, for example, indexing attentional control rather than language specifically, beta values among tasks would be much more similar to one another. The fact that language, but not other domains of cognition such as working memory, executive function, or processing speed emerged as possible explanations for this pattern provide external validity of our resting state measure.

These effects are large for brain-behavior associations. For example,

out of the set of reliably significant effects ($0.02 < B < 0.08$), the largest, MTG/PC1-GA approaches the top-1% mark of brain-wide associations as reported by Marek et al. (2022), i.e. the association approaches the maximally detectable size within Marek et al. As ILI and network laterality are summary measures of functional topology, behavioral associations are naturally larger than those with raw imaging phenotypes.

4.2. Drawbacks to this analysis include task asynchrony and characteristics

One important caveat to note is that there is no straightforward method to quantify the amount of linguistic skills needed for each task, and while the associations between laterality and tasks follow roughly the same pattern between methods, the beta weights do not order in exactly the same way. A second caveat is that, contrary to most imaging analyses of brain organization, we are attempting to draw correlations between observed resting-state organization and task scores completed at another time, which precludes large relationships.

A third major drawback in the present study is that the "language" tasks themselves do not examine more than single words. Toolbox Reading requires proper pronunciations of words presented on a screen and crucially requires no semantic understanding of the stimulus; Toolbox Picture Vocabulary asks the participant to select semantically relevant images following a verbal stimulus, and the RAVLT requires the memorization of loosely semantically organized sets of nouns. In each of these cases, the stimuli are single items, i.e. there is no top-down processing required to understand a sentence or phrase. **We hypothesize that the associations would be larger if tasks that examined higher-order processing skills were analyzed.** However, increasing difficulty may inflate the associations with IFG due to its domain-general role, rather than its linguistic role.

The third area, Wernicke's area, showed no correlation with any behavioral scores. However, given the uncertainty over the existence and role of "Wernicke's area" (Tremblay and Dick, 2016) and the small size of the ROI generated for this analysis may justify this lack of assocation.

As a final point, we approached ROI selection at the population level. We use ROIs constructed from ABCD ARMS 1 that comprise grayordinates that are involved in the VAN in the majority of participants. However, it is possible that IFG or MTG in a given individual is completely or mostly disjoint from this ROI, however, lacking a functional localizer, this approach prioritizes intersubject validity.

5. Conclusions

RS data can be used to calculate coarse measures of hemispheric organization as related to components of the language network. We found that, consistent with earlier work, greater laterality associated with MTG is associated with greater linguistic skills (as measured out of the scanner) in a sample of school-aged children. However, we did not find the same pattern in IFG, which is consistent with more recent work describing IFG as a mosaic of language-selective and task-general regions. We suggest that implementing this technique in other RS data will be fruitful for understanding the development of the language network.

CRediT authorship contribution statement

Elison Jed T.: Funding acquisition, Project administration, Resources, Supervision. **Fair Damien A.:** Funding acquisition, Investigation, Methodology, Project administration, Resources. **Hermosillo Robert J.M.:** Investigation, Methodology, Software. **Conan Gregory:** Methodology, Software. **Feczko Eric:** Conceptualization, Funding acquisition, Investigation, Methodology, Project administration, Resources. **Day Trevor Kincaid McAllister:** Conceptualization, Formal analysis, Funding acquisition, Investigation, Methodology, Visualization, Writing – original draft, Writing – review & editing. **Earl Eric:** Data curation. **Byington Nora:** Data curation. **Randolph Anita:** Methodology, Resources, Software. **Perrone Anders J.:** Data curation. **Hendrickson Timothy J.:** Data curation.

Declaration of Competing Interest

The authors declare that they have no known competing financial interests or personal relationships that could have appeared to influence the work reported in this paper.

Data availability

The neuroimaging and demographic data used in this paper are available through wider efforts to distribute data from the Adolescent Brain and Cognitive Development study. The mixed ROIs, "crossotopes" used in this study are available on Zenodo (https://doi.org/10.1101/2022.01.12.475422), and information about the Hermosillo probabilistic atlases can be found at https://midbatlas.io.

Appendix A. Supporting information

Supplementary data associated with this article can be found in the online version at doi:10.1016/j.dcn.2024.101355.

References

Barch, D.M., Albaugh, M.D., Avenevoli, S., Chang, L., Clark, D.B., Glantz, M.D., Hudziak, J.J., Jernigan, T.L., Tapert, S.F., Yurgelun-Todd, D., Alia-Klein, N., Potter, A.S., Paulus, M.P., Prouty, D., Zucker, R.A., Sher, K.J., 2018. Demographic, physical and mental health assessments in the adolescent brain and cognitive development study: rationale and description. Dev. Cogn. Neurosci. 32, 55–66. https://doi.org/10.1016/j.dcn.2017.10.010.

Bartha-Doering, L., Kollndorfer, K., Kasprian, G., Novak, A., Schuler, A.-L., Fischmeister, F., Ph, S., Alexopoulos, J., Gaillard, W.D., Prayer, D., Seidl, R., Berl, M. M., 2018. Weaker semantic language lateralization associated with better semantic language performance in healthy right-handed children. Brain Behav. 8 (11), e01072 https://doi.org/10.1002/brb3.1072.

Bauer, P.J., Zelazo, P.D., 2014. The national institutes of health toolbox for the assessment of neurological and behavioral function: a tool for developmental science. Child Dev. Perspect. 8 (3), 119–124. https://doi.org/10.1111/cdep.12080.

Bernal, B., Guillen, M., Korman, B., 2018. Nontask-related brain lateralization biomarkers in children: the asymmetry of language areas on functional connectivity functional magnetic resonance imaging. Brain Connect. 8 (6), 321–332.

Bernard, F., Lemee, J.-M., Mazerand, E., Leiber, L.-M., Menei, P., Ter Minassian, A., 2020. The ventral attention network: the mirror of the language network in the right brain hemisphere. J. Anat. 237 (4), 632–642. https://doi.org/10.1111/joa.13223.

Biswal, B., Yetkin, F.Z., Haughton, V.M., Hyde, J.S., 1995. Functional connectivity in the motor cortex of resting human brain using echo-planar mri. Magn. Reson. Med. 34 (4), 537–541. https://doi.org/10.1002/mrm.1910340409.

Bradshaw, A.R., Thompson, P.A., Wilson, A.C., Bishop, D.V.M., Woodhead, Z.V.J., 2017. Measuring language lateralisation with different language tasks: a systematic review. PeerJ 5, e3929. https://doi.org/10.7717/peerj.3929.

Braga, R.M., DiNicola, L.M., Becker, H.C., Buckner, R.L., 2020. Situating the left-lateralized language network in the broader organization of multiple specialized large-scale distributed networks. J. Neurophysiol. 124 (5), 1415–1448. https://doi.org/10.1152/jn.00753.2019.

Branco, P., Seixas, D., Deprez, S., Kovacs, S., Peeters, R., Castro, S.L., Sunaert, S., 2016. Resting-state functional magnetic resonance imaging for language preoperative planning. Front. Hum. Neurosci. 10 https://doi.org/10.3389/fnhum.2016.00011.

Broca, M.P., 1861. Remarques sur le siége de la faculté du langage articulé, suivies d'une observation d'aphémie (perte de la parole). Bull. De. la Société Anat. 18.

Button, K.S., Ioannidis, J.P.A., Mokrysz, C., Nosek, B.A., Flint, J., Robinson, E.S.J., Munafò, M.R., 2013. Power failure: why small sample size undermines the reliability of neuroscience. Article 5. Nat. Rev. Neurosci. 14 (5) https://doi.org/10.1038/nrn3475.

Carrow-Woolfolk, E., 1996. Oral and Written Language Scales. American Guidance Service, Inc.

Casey, B.J., Cannonier, T., Conley, M.I., Cohen, A.O., Barch, D.M., Heitzeg, M.M., Soules, M.E., Teslovich, T., Dellarco, D.V., Garavan, H., Orr, C.A., Wager, T.D., Banich, M.T., Speer, N.K., Sutherland, M.T., Riedel, M.C., Dick, A.S., Bjork, J.M., Thomas, K.M., Imaging Acquisition Workgroup, A.B.C.D., 2018. The adolescent brain cognitive development (ABCD) study: imaging acquisition across 21 sites. Dev. Cogn. Neurosci. 32, 43–54. https://doi.org/10.1016/j.dcn.2018.03.001.

Corbetta, M., Shulman, G.L., 2002. Control of goal-directed and stimulus-driven attention in the brain. Nat. Rev. Neurosci. 3 (3), 201–215. https://doi.org/10.1038/nrn755.

Cosgrove, K.T., McDermott, T.J., White, E.J., Mosconi, M.W., Thompson, W.K., Paulus, M.P., Cardenas-Iniguez, C., Aupperle, R.L., 2022. Limits to the

generalizability of resting-state functional magnetic resonance imaging studies of youth: an examination of ABCD Study® baseline data. Brain Imaging Behav. 16 (4), 1919–1925. https://doi.org/10.1007/s11682-022-00665-2.
Dehaene-Lambertz, G., Dehaene, S., Hertz-Pannier, L., 2002. Functional neuroimaging of speech perception in infants. Science 298 (5600), 2013–2015. https://doi.org/10.1126/science.1077066.
Dick, A.S., Garcia, N.L., Pruden, S.M., Thompson, W.K., Hawes, S.W., Sutherland, M.T., Riedel, M.C., Laird, A.R., Gonzalez, R., 2019. No evidence for a bilingual executive function advantage in the ABCD study. Article 7. Nat. Hum. Behav. 3 (7) https://doi.org/10.1038/s41562-019-0609-3.
Dubois, J., Alison, M., Counsell, S.J., Hertz-Pannier, L., Hüppi, P.S., Benders, M.J.N.L., 2021. MRI of the neonatal brain: a review of methodological challenges and neuroscientific advances. J. Magn. Reson. Imaging 53 (5), 1318–1343. https://doi.org/10.1002/jmri.27192.
Ebert, S., Peterson, C., Slaughter, V., Weinert, S., 2017. Links among parents' mental state language, family socioeconomic status, and preschoolers' theory of mind development. Cogn. Dev. 44, 32–48. https://doi.org/10.1016/j.cogdev.2017.08.005.
Enge, A., Friederici, A.D., Skeide, M.A., 2020. A meta-analysis of fMRI studies of language comprehension in children. NeuroImage 215, 116858. https://doi.org/10.1016/j.neuroimage.2020.116858.
Everts, R., Lidzba, K., Wilke, M., Kiefer, C., Mordasini, M., Schroth, G., Perrig, W., Steinlin, M., 2009. Strengthening of laterality of verbal and visuospatial functions during childhood and adolescence. Hum. Brain Mapp. 30 (2), 473–483. https://doi.org/10.1002/hbm.20523.
Feczko, E., Conan, G., Marek, S., Tervo-Clemmens, B., Cordova, M., Doyle, O., Earl, E., Perrone, A., Sturgeon, D., Klein, R., Harman, G., Kilamovich, D., Hermosillo, R., Miranda-Dominguez, O., Adebimpe, A., Bertolero, M., Cieslak, M., Covitz, S., Hendrickson, T., … Fair, D.A. (2021). Adolescent Brain Cognitive Development (ABCD) Community MRI Collection and Utilities (p. 2021.07.09.451638). bioRxiv. https://doi.org/10.1101/2021.07.09.451638.
Fedorenko, E., Blank, I.A., 2020. Broca's area is not a natural kind. Trends Cogn. Sci. 24 (4), 270–284. https://doi.org/10.1016/j.tics.2020.01.001.
Flinker, A., Korzeniewska, A., Shestyuk, A.Y., Franaszczuk, P.J., Dronkers, N.F., Knight, R.T., Crone, N.E., 2015. Redefining the role of Broca's area in speech. Proc. Natl. Acad. Sci. USA 112 (9), 2871–2875. https://doi.org/10.1073/pnas.1414491112.
Fransson, P., Åden, U., Blennow, M., Lagercrantz, H., 2011. The functional architecture of the infant brain as revealed by resting-state fMRI. Cereb. Cortex 21 (1), 145–154. https://doi.org/10.1093/cercor/bhq071.
Gao, W., Zhu, H., Giovanello, K.S., Smith, J.K., Shen, D., Gilmore, J.H., Lin, W., 2009. Evidence on the emergence of the brain's default network from 2-week-old to 2-year-old healthy pediatric subjects. Proc. Natl. Acad. Sci. 106 (16), 6790–6795. https://doi.org/10.1073/pnas.0811221106.
Gao, W., Lin, W., Grewen, K., Gilmore, J.H., 2017. Functional connectivity of the infant human brain: plastic and modifiable. Neuroscientist 23 (2), 169–184. https://doi.org/10.1177/1073858416635986.
Gordon, E.M., Laumann, T.O., Adeyemo, B., Huckins, J.F., Kelley, W.M., Petersen, S.E., 2016. Generation and evaluation of a cortical area parcellation from resting-state correlations. Cereb. Cortex 26 (1), 288–303. https://doi.org/10.1093/cercor/bhu239.
Gordon, E.M., Laumann, T.O., Adeyemo, B., Gilmore, A.W., Nelson, S.M., Dosenbach, N.U.F., Petersen, S.E., 2017. Individual-specific features of brain systems identified with resting state functional correlations. NeuroImage 146, 918–939. https://doi.org/10.1016/j.neuroimage.2016.08.032.
Hermosillo, R.J.M., Moore, L.A., Fezcko, E., Dworetsky, A., Pines, A., Conan, G., Mooney, M.A., Randolph, A., Adeyemo, B., Earl, E., Perrone, A., Carrasco, C.M., Uriarte-Lopez, J., Snider, K., Doyle, O., Cordova, M., Nagel, B.J., Ewing, S.W.F., Satterthwaite, T., … Fair, D.A., 2022. A Precision Functional Atlas of Network Probabilities and Individual-Specific Network Topography (p. 2022.01.12.475422). bioRxiv. https://doi.org/10.1101/2022.01.12.475422.
Hermundstad, A.M., Bassett, D.S., Brown, K.S., Aminoff, E.M., Clewett, D., Freeman, S., Frithsen, A., Johnson, A., Tipper, C.M., Miller, M.B., Grafton, S.T., Carlson, J.M., 2013. Structural foundations of resting-state and task-based functional connectivity in the human brain. Proc. Natl. Acad. Sci. 110 (15), 6169–6174. https://doi.org/10.1073/pnas.1219562110.
Hervé, P.-Y., Zago, L., Petit, L., Mazoyer, B., Tzourio-Mazoyer, N., 2013. Revisiting human hemispheric specialization with neuroimaging. Trends Cogn. Sci. 17 (2), 69–80. https://doi.org/10.1016/j.tics.2012.12.004.
Hillis, A.E., Work, M., Barker, P.B., Jacobs, M.A., Breese, E.L., Maurer, K., 2004. Re-examining the brain regions crucial for orchestrating speech articulation. Brain 127 (7), 1479–1487. https://doi.org/10.1093/brain/awh172.
Holland, S.K., Vannest, J., Mecoli, M., Jacola, L.M., Tillema, J.-M., Karunanayaka, P.R., Schmithorst, V.J., Yuan, W., Plante, E., Byars, A.W., 2007. Functional MRI of language lateralization during development in children. Int. J. Audiol. 46 (9), 533–551. https://doi.org/10.1080/14992020701448994.
Howell, B.R., Styner, M.A., Gao, W., Yap, P.-T., Wang, L., Baluyot, K., Yacoub, E., Chen, G., Potts, T., Salzwedel, A., Li, G., Gilmore, J.H., Piven, J., Smith, J.K., Shen, D., Ugurbil, K., Zhu, H., Lin, W., Elison, J.T., 2018. The UNC/UMN baby connectome project (BCP): an overview of the study design and protocol development. NeuroImage 185, 891–905. https://doi.org/10.1016/j.neuroimage.2018.03.049.
Hwang, G., Dabbs, K., Conant, L., Nair, V.A., Mathis, J., Almane, D.N., Nencka, A., Birn, R., Humphries, C., Raghavan, M., DeYoe, E.A., Struck, A.F., Maganti, R., Binder, J.R., Meyerand, E., Prabhakaran, V., Hermann, B., 2019. Cognitive slowing and its underlying neurobiology in temporal lobe epilepsy. Cortex 117, 41–52. https://doi.org/10.1016/j.cortex.2019.02.022.
Johnson, M.H., 2001. Functional brain development in humans. Article 7. Nat. Rev. Neurosci. 2 (7) https://doi.org/10.1038/35081509.
Joliot, M., Tzourio-Mazoyer, N., Mazoyer, B., 2016. Intra-hemispheric intrinsic connectivity asymmetry and its relationships with handedness and language Lateralization. Neuropsychologia 93, 437–447.
Keller, A.S., Pines, A.R., Sydnor, V.J., Cui, Z., Bertolero, M.A., Barzilay, R., Alexander-Bloch, A., Byington, N., Chen, A.A., Conan, G.M.2022. Personalized Functional Brain Network Topography Predicts Individual Differences in Youth Cognition. bioRxiv, 2022–10.
Korom, M., Camacho, M.C., Filippi, C.A., Licandro, R., Moore, L.A., Dufford, A., Zöllei, L., Graham, A.M., Spann, M., Howell, B., Shultz, S., Scheinost, D., 2022. Dear reviewers: responses to common reviewer critiques about infant neuroimaging studies. Dev. Cogn. Neurosci. 53, 101055 https://doi.org/10.1016/j.dcn.2021.101055.
Lee, M.H., Hacker, C.D., Snyder, A.Z., Corbetta, M., Zhang, D., Leuthardt, E.C., Shimony, J.S., 2012. Clustering of resting state networks. PLOS ONE 7 (7), e40370. https://doi.org/10.1371/journal.pone.0040370.
Lezak, M.D., 1983. Neuropsychological assessment, 2nd ed..,. Oxford University Press.
Lidzba, K., Schwilling, E., Grodd, W., Krägeloh-Mann, I., Wilke, M., 2011. Language comprehension vs. language production: age effects on fMRI activation. Brain Lang. 119 (1), 6–15. https://doi.org/10.1016/j.bandl.2011.02.003.
Lipkin, B., Tuckute, G., Affourtit, J., Small, H., Mineroff, Z., Kean, H., Jouravlev, O., Rakocevic, L., Pritchett, B., Siegelman, M., Hoeflin, C., Pongos, A., Blank, I.A., Struhl, M.K., Ivanova, A., Shannon, S., Sathe, A., Hoffmann, M., Nieto-Castañón, A., Fedorenko, E., 2022. LanA (Language Atlas): A probabilistic atlas for the language network based on fMRI data from >800 individuals (p. 2022.03.06.483177). bioRxiv. https://doi.org/10.1101/2022.03.06.483177.
Long, M.A., Katlowitz, K.A., Svirsky, M.A., Clary, R.C., Byun, T.M., Majaj, N., Oya, H., Howard, M.A., Greenlee, J.D.W., 2016. Functional segregation of cortical regions underlying speech timing and articulation. Neuron 89 (6), 1187–1193. https://doi.org/10.1016/j.neuron.2016.01.032.
Marek, S., Tervo-Clemmens, B., Calabro, F.J., Montez, D.F., Kay, B.P., Hatoum, A.S., Donohue, M.R., Foran, W., Miller, R.L., Hendrickson, T.J., Malone, S.M., Kandala, S., Feczko, E., Miranda-Dominguez, O., Graham, A.M., Earl, E.A., Perrone, A.J., Cordova, M., Doyle, O., Dosenbach, N.U.F., 2022. Reproducible brain-wide association studies require thousands of individuals. Nature 603 (7902), 654–660. https://doi.org/10.1038/s41586-022-04492-9.
Mennes, M., Kelly, C., Zuo, X.-N., Di Martino, A., Biswal, B.B., Castellanos, F.X., Milham, M.P., 2010. Inter-individual differences in resting-state functional connectivity predict task-induced BOLD activity. NeuroImage 50 (4), 1690–1701. https://doi.org/10.1016/j.neuroimage.2010.01.002.
Monopoli, W.J., Kingston, S., 2012. The relationships among language ability, emotion regulation and social competence in second-grade students. Int. J. Behav. Dev. 36 (5), 398–405. https://doi.org/10.1177/0165025412446394.
Moore, L.A., Hermosillo, R.J., Feczko, E., Moser, J., Koirala, S., Allen, M.C., Buss, C., Conan, G., Juliano, A.C., Marr, M., Miranda-Dominguez, O., Mooney, M., Myers, M., Rasmussen, J., Rogers, C., Smyser, C., Snider, K., Sylvester, C., Thomas, E., … Graham, A.M. , 2023. *Towards Personalized Precision Functional Mapping in Infancy* (SSRN Scholarly Paper 4428815). https://doi.org/10.2139/ssrn.4428815.
Mungas, D., Widaman, K., Zelazo, P.D., Tulsky, D., Heaton, R.K., Slotkin, J., Blitz, D.L., Gershon, R.C., 2013. VII. NIH toolbox cognition battery (CB): factor structure for 3 to 15 year olds. Monogr. Soc. Res. Child Dev. 78 (4), 103–118. https://doi.org/10.1111/mono.12037.
Olman, C.A., Davachi, L., Inati, S., 2009. Distortion and signal loss in medial temporal lobe. PLoS ONE 4 (12), e8160. https://doi.org/10.1371/journal.pone.0008160.
Olulade, O.A., Seydell-Greenwald, A., Chambers, C.E., Turkeltaub, P.E., Dromerick, A.W., Berl, M.M., Gaillard, W.D., Newport, E.L., 2020. The neural basis of language development: changes in lateralization over age. Proc. Natl. Acad. Sci. 117 (38), 23477–23483. https://doi.org/10.1073/pnas.1905590117.
Papoutsi, M., de Zwart, J.A., Jansma, J.M., Pickering, M.J., Bednar, J.A., Horwitz, B., 2009. From phonemes to articulatory codes: an fMRI study of the role of Broca's area in speech production. Cereb. Cortex 19 (9), 2156–2165. https://doi.org/10.1093/cercor/bhn239.
Perani, D., Saccuman, M.C., Scifo, P., Anwander, A., Spada, D., Baldoli, C., Poloniato, A., Lohmann, G., Friederici, A.D., 2011. Neural language networks at birth. Proc. Natl. Acad. Sci. 108 (38), 16056–16061. https://doi.org/10.1073/pnas.1102991108.
Petitto, L.A., Berens, M.S., Kovelman, I., Dubins, M.H., Jasinska, K., Shalinsky, M., 2012. The "perceptual wedge hypothesis" as the basis for bilingual babies' phonetic processing advantage: new insights from fNIRS brain imaging. Brain Lang. 121 (2), 130–143. https://doi.org/10.1016/j.bandl.2011.05.003.
Poldrack, R.A., Baker, C.I., Durnez, J., Gorgolewski, K.J., Matthews, P.M., Munafò, M.R., Nichols, T.E., Poline, J.-B., Vul, E., Yarkoni, T., 2017. Scanning the horizon: towards transparent and reproducible neuroimaging research. Article 2. Nat. Rev. Neurosci. 18 (2) https://doi.org/10.1038/nrn.2016.167.
Power, J.D., Cohen, A.L., Nelson, S.M., Wig, G.S., Barnes, K.A., Church, J.A., Vogel, A.C., Laumann, T.O., Miezin, F.M., Schlaggar, B.L., Petersen, S.E., 2011. Functional network organization of the human brain. Neuron 72 (4), 665–678. https://doi.org/10.1016/j.neuron.2011.09.006.
Ratcliff, G., 1979. Spatial thought, mental rotation and the right cerebral hemisphere. Neuropsychologia 17 (1), 49–54. https://doi.org/10.1016/0028-3932(79)90021-6.
Sepeta, L.N., Berl, M.M., Wilke, M., You, X., Mehta, M., Xu, B., Inati, S., Dustin, I., Khan, O., Austermuehle, A., Theodore, W.H., Gaillard, W.D., 2016. Age-dependent mesial temporal lobe lateralization in language fMRI. Epilepsia 57 (1), 122–130. https://doi.org/10.1111/epi.13258.

Shing, Y.L., Lindenberger, U., Diamond, A., Li, S.-C., Davidson, M.C., 2010. Memory maintenance and inhibitory control differentiate from early childhood to adolescence. Dev. Neuropsychol. 35 (6), 679–697. https://doi.org/10.1080/87565641.2010.508546.

Skeide, M.A., Friederici, A.D., 2016. The ontogeny of the cortical language network. Article 5. Nat. Rev. Neurosci. 17 (5) https://doi.org/10.1038/nrn.2016.23.

Skeide, M.A., Brauer, J., Friederici, A.D., 2014. Syntax gradually segregates from semantics in the developing brain. NeuroImage 100, 106–111. https://doi.org/10.1016/j.neuroimage.2014.05.080.

Smitha, K.A., Arun, K.M., Rajesh, P.G., Thomas, B., Kesavadas, C., 2017. Resting-state seed-based analysis: an alternative to task-based language fMRI and its laterality index. Am. J. Neuroradiol. 38 (6), 1187–1192. https://doi.org/10.3174/ajnr.A5169.

Smitha, K.A., Arun, K.M., Rajesh, P.G., Thomas, B., Radhakrishnan, A., Sarma, P.S., Kesavadas, C., 2019. Resting fMRI as an alternative for task-based fMRI for language lateralization in temporal lobe epilepsy patients: a study using independent component analysis. Neuroradiology 61, 803–810. https://doi.org/10.1007/s00234-019-02209-w.

Sturgeon, D., Earl, E., Perrone, A., Snider, K., 2021. DCAN-Labs/abcd-hcp-pipeline: minor update to DCAN BOLD Processing and MRE version [Computer software]. Zenodo. https://doi.org/10.5281/zenodo.4571051.

Szaflarski, J.P., Holland, S.K., Schmithorst, V.J., Byars, A.W., 2006. An fMRI study of language lateralization in children and adults. Hum. Brain Mapp. https://doi.org/10.1002/hbm.20177.

Szaflarski, J.P., Schmithorst, V.J., Altaye, M., Byars, A.W., Ret, J., Plante, E., Holland, S. K., 2006. A longitudinal fMRI study of language development in children age 5–11. Ann. Neurol. https://doi.org/10.1002/ana.20817.

Tavor, I., Jones, O.P., Mars, R.B., Smith, S.M., Behrens, T.E., Jbabdi, S., 2016. Task-free MRI predicts individual differences in brain activity during task performance. Science 352 (6282), 216–220. https://doi.org/10.1126/science.aad8127.

Thompson, W.K., Barch, D.M., Bjork, J.M., Gonzalez, R., Nagel, B.J., Nixon, S.J., Luciana, M., 2019. The structure of cognition in 9 and 10 year-old children and associations with problem behaviors: findings from the ABCD study's baseline neurocognitive battery. Dev. Cogn. Neurosci. 36, 100606 https://doi.org/10.1016/j.dcn.2018.12.004.

Tremblay, P., Dick, A.S., 2016. Broca and Wernicke are dead, or moving past the classic model of language neurobiology. Brain Lang. 162, 60–71. https://doi.org/10.1016/j.bandl.2016.08.004.

Tzourio-Mazoyer, N., Joliot, M., Marie, D., Mazoyer, B., 2016. Variation in homotopic areas' activity and inter-hemispheric intrinsic connectivity with type of language lateralization: An FMRI study of covert sentence generation in 297 healthy volunteers. Brain Struct. Funct. 221, 2735–2753. https://doi.org/10.1007/s00429-015-1068-x.

Veale, J.F., 2014. Edinburgh handedness inventory - short form: a revised version based on confirmatory factor analysis. Laterality 19 (2), 164–177. https://doi.org/10.1080/1357650X.2013.783045.

Volkow, N.D., Koob, G.F., Croyle, R.T., Bianchi, D.W., Gordon, J.A., Koroshetz, W.J., Pérez-Stable, E.J., Riley, W.T., Bloch, M.H., Conway, K., Deeds, B.G., Dowling, G.J., Grant, S., Howlett, K.D., Matochik, J.A., Morgan, G.D., Murray, M.M., Noronha, A., Spong, C.Y., Weiss, S.R.B., 2018. The conception of the ABCD study: from substance use to a broad NIH collaboration. Dev. Cogn. Neurosci. 32, 4–7. https://doi.org/10.1016/j.dcn.2017.10.002.

Wechsler, D., 2014. *Wechsler Adult Intelligence Scale (WAISIV)* (4th ed.).

Weintraub, S., Bauer, P.J., Zelazo, P.D., Wallner-Allen, K., Dikmen, S.S., Heaton, R.K., Tulsky, D.S., Slotkin, J., Blitz, D.L., Carlozzi, N.E., Havlik, R.J., Beaumont, J.L., Mungas, D., Manly, J.J., Borosh, B.G., Nowinski, C.J., Gershon, R.C., 2013. I. NIH toolbox cognition battery (CB): introduction and pediatric data. Monogr. Soc. Res. Child Dev. 78 (4), 1–15. https://doi.org/10.1111/mono.12031.

Weiss-Croft, L.J., Baldeweg, T., 2015. Maturation of language networks in children: a systematic review of 22years of functional MRI. NeuroImage 123, 269–281. https://doi.org/10.1016/j.neuroimage.2015.07.046.

Yeo, B.T.T., Krienen, F.M., Sepulcre, J., Sabuncu, M.R., Lashkari, D., Hollinshead, M., Roffman, J.L., Smoller, J.W., Zöllei, L., Polimeni, J.R., Fischl, B., Liu, H., Buckner, R. L., 2011. The organization of the human cerebral cortex estimated by intrinsic functional connectivity. J. Neurophysiol. 106 (3), 1125–1165. https://doi.org/10.1152/jn.00338.2011.

Zago, L., Petit, L., Mellet, E., Jobard, G., Crivello, F., Joliot, M., Mazoyer, B., Tzourio-Mazoyer, N., 2016. The association between hemispheric specialization for language production and for spatial attention depends on left-hand preference strength. Neuropsychologia 93, 394–406.